Condensed matter physics in the 21st century: The legacy of Jacques Friedel

Rapid magnetic oscillations and magnetic breakdown in quasi-1D conductors

Oscillations magnétiques rapides et rupture magnétique dans les conducteurs quasi-1D

Gilles Montambaux, Denis Jérome

Laboratoire de physique des solides, CNRS UMR 8502, Université Paris-Sud, 91405 Orsay cedex, France

ABSTRACT

We review the physics of magnetic quantum oscillations in quasi-one dimensional conductors with an open Fermi surface, in the presence of modulated order. We emphasize the difference between situations where a modulation couples states on the *same* side of the Fermi surface and a modulation couples states on *opposite* sides of the Fermi surface. We also consider cases where several modulations coexist, which may lead to a complex reorganization of the Fermi surface. The interplay between nesting effects and magnetic breakdown is discussed. The experimental situation is reviewed.

© 2015 Académie des sciences. Published by Elsevier Masson SAS. This is an open access article under the CC BY-NC-ND license (http://creativecommons.org/licenses/by-nc-nd/4.0/).

RÉSUMÉ

Cet article est une revue sur les oscillations quantiques magnétiques dans les conducteurs quasi-unidimensionnels avec une surface de Fermi ouverte, en présence d'un potentiel périodique extérieur. On insiste sur la différence entre les cas où une telle modulation couple des états du *même côté* de la surface de Fermi et où cette modulation couple des états *sur des branches différentes* de la surface de Fermi. On considère aussi des cas où plusieurs modulations coexistent, ce qui conduit à une réorganisation complexe de la surface de Fermi. On discute la compétition entre effets de nesting et rupture magnétique. On termine par une revue de la situation expérimentale.

© 2015 Académie des sciences. Published by Elsevier Masson SAS. This is an open access article under the CC BY-NC-ND license (http://creativecommons.org/licenses/by-nc-nd/4.0/).

1. Introduction

It is well known that magnetic oscillations in thermodynamic and transport properties originate from the Landau quantization of *closed* electronic orbits. The existence of such oscillations in quasi-1D conductors with an *open* Fermi Surface (FS), especially studied in compounds of the Bechgaard salts family, has thus been a long standing problem (for a review, see Refs. [1,2]). Various mechanisms have been invoked to explain the existence of these quantum oscillations in the presence
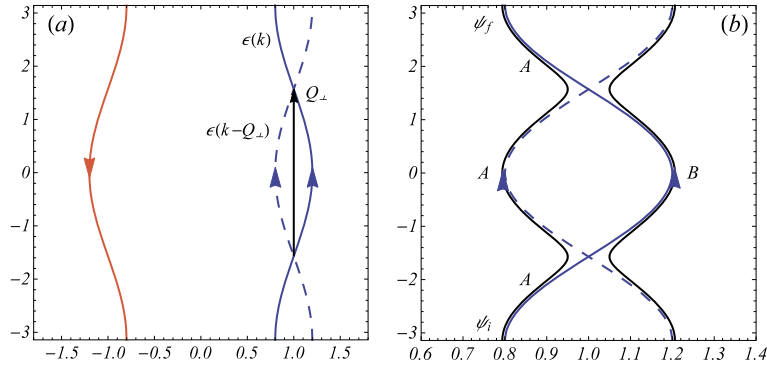
Fig. 1. a) A modulation at a transverse wave vector $\mathbf{Q}_\perp = (0, \pi/b)$ couples states on the same side of the FS. In a magnetic field, the coupled trajectories (blue and dashed blue) flow along the same direction. b) The opening of a gap creates two open warped sheets of the FS (black), with the possibility magnetic breakdown at $(k_F, \pm\pi/(2b))$. An electron initially on the sheet A may travel along two interfering paths (AAA and ABA), leading to magnetic oscillations in the conductance, with a frequency proportional to t_b. (For interpretation of the references to colour in this figure, the reader is referred to the web version of this article.)

of open orbits. Most of them are based on the existence of an external periodic potential which permits a modification of the Fermi surface. Other mechanisms like the magnetic field modulation of electron–electron scattering [3] and the rich physics of the angular oscillations are not discussed here [2].

One of these mechanisms is the Density Wave (DW) ordering due to almost perfect nesting of the Fermi surface (FS). Such ordering leaves small *closed* electronic pockets of unpaired carriers, the size of which is related to the deviation from perfect nesting, as recalled later in this paper (Fig. 5). In a magnetic field B applied along a direction perpendicular to the most conducting planes, the quantization of the electronic motion along these closed pockets leads to Shubnikov–de Haas (SdH) oscillations (periodic in $1/B$) the period of which is proportional to the size of the pocket. The typical field B_f characteristic of the oscillations is proportional to the area $\mathcal{A}$ of the closed orbits in reciprocal space $B_f = \frac{\hbar}{2\pi e}\mathcal{A}$. The characteristic energy of deviation from perfect nesting, named t_b', is usually of the order of 10–30 K, so that $\mathcal{A} \propto \frac{t_b'}{\hbar v_F b}$, and the typical field $B_f \propto \frac{t_b'}{e v_F b}$ is of the order of a few dozen teslas. In Bechgaard salts, the competition between Spin Density Wave (SDW) ordering and the quantization due to the magnetic field leads to a cascade of SDW subphases, in which the Hall effect is quantized [1,2,4–6].

In this paper, we focus our study on the understanding of the so-called *Rapid Oscillations* (ROs), described by a much larger characteristic field, of the order of a few hundred teslas, believed to be related to the typical warping of the FS related to an energy scale $t_b \gg t_b'$; ($\mathcal{A} \propto \frac{t_b}{\hbar v_F b}$ and $B_f \propto \frac{t_b}{e v_F b}$). This corresponds to much larger orbits which cannot be explained by DW ordering alone.

We examine various kinds of external periodic potentials that may give rise to such rapid oscillations. We consider a simple band model in order to study the effect of different modulations on the electronic spectrum and their consequence on the structure of the magnetic-field-induced quantum oscillations. We start from the widely used two-dimensional tight-binding model describing a metallic phase with a simple orthorhombic dispersion with hopping parameters t_a along the x direction of the conducting chains and t_b along the perpendicular y direction. The magnetic field is applied along the z direction (the c^* direction in Bechgaard salts having triclinic symmetry). The dispersion relation may be linearized along the high conductivity direction and the modulation along the transverse direction is then described by two harmonics with amplitudes t_b and t_b' [1,2,4,5]:

$$\epsilon_{\boldsymbol{k}} = \epsilon_F + \hbar v_F(|k_x| - k_F) - 2t_b \cos k_y b - 2t_b' \cos 2k_y b \tag{1}$$

We take the Fermi energy $\epsilon_F = 2t_a \cos k_F a$ as the origin of the energies and the Fermi velocity v_F is given by $\hbar v_F = 2t_a a \sin k_F a$. The corresponding FS is made of two warped sheets located at $\pm k_F$ (Fig. 1-a). The amplitude of the warping is given by t_b. As we will recall in section 5, a wave vector $\mathbf{Q}_N = (2k_F, \pi/b)$ almost perfectly nests the two sheets.[1] The deviation from perfect nesting is then related to the amplitude t_b'.

In this paper, we emphasize the possible existence of two different kinds of periodic structural modulations and their consequences on the structure of the FS and on the nature of the magnetic oscillations.

i) *Modulations with wave vector along the transverse direction to the conducting chains* (Fig. 1). A modulation at wave vector $\mathbf{Q}_\perp = (0, \pi/b)$ couples electronic states located on the *same* side of the FS. In a magnetic field, two *open* trajectories flow along the *same direction* and may interfere at special positions in reciprocal space, realizing a double-path interferometer [7].

ii) *Modulations the wave vector of which has a $2k_F$ component which couples states located on opposite sides of the FS* (Fig. 4). A modulation at wave vector $\mathbf{Q}_\parallel = (2k_F, 0)$ opens a gap at a transverse position $\pm\pi/(2b)$ and leaves *closed* orbits of size

---

[1] The best nesting vector is actually slightly different from this commensurate value.

proportional to the energy scale t_b. Quantization of these closed orbits in a magnetic field leads to Shubnikov–de Haas (SdH) oscillations, the frequency of which is proportional to t_b.

As shown in Figs. 1, 4, the dynamics in a magnetic field is quite different between that in these two cases, since in the first case, the coupled trajectories have the *same* direction in a magnetic field, while in the second case they follow *opposite* directions.

The present work is motivated by several puzzling experiments showing rapid oscillations (frequency t_b) performed in Bechgaard salts. The next section presents a brief overview of these experiments. Then we consider different situations corresponding to different modulations. The main goal of the present paper is not to address in detail a given experiment, but rather to show the variety of the possible mechanisms. Whenever it looks appropriate, we refer to a given experimental result. The outline is the following. In section 3, we consider a transverse modulation ($\mathbf{Q}_\perp$) that connects states on the same side of the FS. This modulation induces a pair of trajectories that may interfere in a magnetic field through Magnetic Breakdown (MB) [7]. This interference effect is reminiscent of the Stückelberg oscillations between two Landau–Zener transitions [8]. In section 4, we consider a longitudinal modulation ($\mathbf{Q}_\parallel$), which naturally produces closed orbits of the appropriate size to induce rapid quantum oscillations. For these two cases, we calculate explicitly the variation of the characteristic field B_f with the amplitude of the gap induced by the modulation in the electronic spectrum. Section 5 recalls the case of almost perfect nesting induced by a DW ($\mathbf{Q}_N$), which leads to small pockets and slow oscillations. Then we consider situations where *two modulations coexist* ($\mathbf{Q}_N$ and $\mathbf{Q}_\perp$ in section 6; $\mathbf{Q}_N$ and $\mathbf{Q}_\parallel$ in section 7). Such a coexistence leads to a more complex structure of the Fermi pockets in the ordered phase. A similar mechanism may occur in a triclinic crystal where the two sheets are translated with respect to each other, so that naturally two DWs may coexist. This is discussed in section 8. We then conclude on the experimental situation.

2. Experimental overview

We start with an overview of the experiments showing quantum oscillations in the quasi-1D conductors and restrict ourselves to the members of the Bechgaard salts (TMTSF)$_2$X family and describe the two kinds of oscillatory behaviours (periodic in $1/B$) that have been observed.

In (TMTSF)$_2$ClO$_4$ [9–11], (TMTSF)$_2$PF$_6$ [12,13], and (TMTSF)$_2$ReO$_4$ under pressure [14], oscillations with a frequency around 30 T (the so-called *slow oscillations*) are observed at low temperature when the metallic phase is stable *albeit* above a threshold magnetic field $\approx$5–8 T [15,16]. These oscillations are now fairly well understood in terms of the stabilization of field-induced spin density wave phases (FISDW) [5] and will not be discussed in this paper.

Quite an intriguing feature is the observation of oscillations with a much higher characteristic frequency, typically 250–300 T, the so-called *Rapid Oscillations* (ROs) in the ambient pressure SDW phase of (TMTSF)$_2$PF$_6$ [13] and (TMTSF)$_2$AsF$_6$ [17,18], in the high magnetic field ($N = 0$) FISDW of (TMTSF)$_2$ClO$_4$ [19] and (TMTSF)$_2$PF$_6$ under pressure [20], and even in the SDW phase of rapidly cooled (quenched: Q) Q-(TMTSF)$_2$ClO$_4$ at ambient pressure [18]. They are also observed in the metallic phase of slowly cooled (relaxed: R) R-(TMTSF)$_2$ClO$_4$ at ambient pressure [11,19,21], and (TMTSF)$_2$ReO$_4$ under pressure [14].

The salt (TMTSF)$_2$NO$_3$ is somewhat peculiar, since slow and rapid oscillations are observed in the ambient pressure SDW phase under low and high fields, respectively [22]. When the SDW phase is suppressed under a pressure exceeding 8 kbar [23], ROs are the only oscillations that survive [24,25].

From these observations, we may draw three important conclusions. i) The analysis of ROs in all four compounds ClO$_4$, PF$_6$, ReO$_4$, NO$_3$ shows that their existence is not necessarily related to the FISDW phases. ii) The frequency of these rapid oscillations is related to interchain coupling t_b, that is to the warping of the open Fermi surface. iii) In several cases the temperature dependence of the amplitude exhibits a marked deviation from the conventional Lifshitz–Kosevich description, especially a sudden vanishing of the oscillations at low temperature [18]. Guided by these observations, we now propose an overview of all situations where ROs arise in these materials with a unified theoretical model based on the experimental results.

3. Transverse $(0, \pi/b)$ modulation

We first consider the existence of a transverse modulation with amplitude $\Delta_\perp$ at wave vector $\mathbf{Q}_\perp = (0, \pi/b)$, as could be induced by an anion modulation along the transverse y direction created by the ordering of ClO$_4$ anions in (TMTSF)$_2$ClO$_4$. The modulation couples states on the *same* side of the FS (Fig. 1).

In the presence of a magnetic field B, the electrons experience a motion along an open FS and quantum oscillations are usually not expected for an open FS. However, the situation is different here since *two* open trajectories run at short distance in $\mathbf{k}$ space and magnetic breakdown near the points $(k_F, \pm\pi/2b)$ is possible [7,19,26].

The potential $\Delta_\perp$ couples $|\mathbf{k}\rangle$ and $|\mathbf{k} - \mathbf{Q}_\perp\rangle$, that is states on the *same* side of the Fermi surface. For $k_x > 0$, this coupling is described by the effective Hamiltonian

$$\mathcal{H}_A(\mathbf{k}) = \begin{pmatrix} \epsilon_{\mathbf{k}} & \Delta_\perp \\ \Delta_\perp & \epsilon_{\mathbf{k} - \mathbf{Q}_\perp} \end{pmatrix} \tag{2}$$

with $\epsilon_{\mathbf{k}}$ given by (1) and

$$\epsilon_{\boldsymbol{k}-\boldsymbol{Q}_\perp} = \hbar v_F(k_x - k_F) + 2t_b \cos k_y b - 2t'_b \cos 2k_y b \tag{3}$$

The t'_b term only slightly distorts the FS, but does not change the physics at all. Therefore, we set here $t'_b = 0$. The new spectrum is given by

$$E_{\boldsymbol{k}} = \hbar v_F(k_x - k_F) \pm \sqrt{\Delta_\perp^2 + 4t_b^2 \cos^2 k_y b} \tag{4}$$

and the equation of the corresponding FS ($E_{\boldsymbol{k}} = 0$) is

$$k_x = k_F \pm \frac{1}{\hbar v_F}\sqrt{4t_b^2 \cos^2 k_y b + \Delta_\perp^2} \tag{5}$$

It is shown in Fig. 1. It consists of two warped sheets along the same side of the FS.

3.1. Open orbits and magnetic breakdown

We estimate now the probability of magnetic breakdown in the vicinity of the gap separating these two sheets. Near the Bragg reflexion $k_y = \pm\pi/(2b)$, and expanding $k_y = \xi\pi/(2b) + q_y$ with $\xi = \pm 1$, the Hamiltonian has the form:

$$\mathcal{H}_A(q_y) = \begin{pmatrix} 2\xi t_b b q_y & \Delta_\perp \\ \Delta_\perp & -2\xi t_b b q_y \end{pmatrix} \tag{6}$$

with the spectrum

$$E_{\boldsymbol{k}} = \pm\sqrt{\Delta_\perp^2 + 4t_b^2 b^2 q_y^2} \tag{7}$$

We define the transverse velocity as $\hbar v_y = 2t_b b$. In a magnetic field B, the transverse wave vector q_y varies linearly with the field, due to the Lorentz force $F = e v_F B$

$$\hbar q_y = e v_F B t \tag{8}$$

so that the time-dependent Hamiltonian simply reads

$$\mathcal{H}_A(t) = \begin{pmatrix} \xi v_y F t & \Delta_\perp \\ \Delta_\perp & -\xi v_y F t \end{pmatrix} \tag{9}$$

This problem is exactly equivalent to the Landau–Zener problem associated with the one-dimensional adiabatic spectrum [27]:

$$E(t) = \pm\sqrt{\Delta_\perp^2 + v_y^2 F^2 t^2} \tag{10}$$

It is known that in this case, the Landau–Zener probability is therefore given by (the gap being $2\Delta_\perp$) [27]:

$$p_\perp \equiv e^{-2\pi\delta} = e^{-\pi \frac{\Delta_\perp^2}{\hbar v_y F}} \tag{11}$$

δ is called the adiabaticity parameter. In our case, the MB probability is given by

$$p_\perp = e^{-\frac{B_\perp}{B}} \quad \text{with} \quad B_\perp = \pi\frac{\Delta_\perp^2}{e\hbar v_y v_F} = \frac{\pi}{2}\frac{\Delta_\perp^2}{e t_b b v_F} \tag{12}$$

which is of the form found in Schoenberg (Eq. (7.13)) [28,29]. At this stage, it is useful to compare this result with similar but different formulas used in the literature for $p_\perp$. In Ref. [19], Uji et al. address the rapid oscillations in $(TMTST)_2ClO_4$. The ROs in the metallic phase are attributed to the Stark–Stückelberg mechanism that we discuss below. The characteristic field for magnetic breakdown is evaluated as $B_\perp = \frac{\Delta_\perp^2 m_c}{\hbar e \epsilon_F}$, where m_c is a cyclotron effective mass defined as $m_c = \hbar/(e v_F b)$ and assumed to be of the order of the free electron's mass. Our result disagrees with this estimate since the energy scale in the denominator is proportional to t_b and not to $\epsilon_F \propto t_a$. In Ref. [26], a slightly more refined formula $B_\perp = \frac{\Delta_\perp^2 m^*}{\hbar e \epsilon_F \sin(2\theta)}$ is in qualitative agreement with our result since θ is defined as the scattering angle at the gap, and is therefore of the order of t_b/t_a.
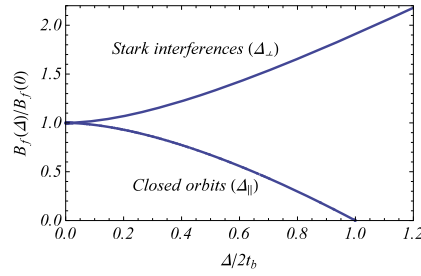
Fig. 2. Gap dependence of the characteristic field B_f of the rapid oscillations, for a transverse modulation $\Delta_\perp$ leading to Stark interferences and for a longitudinal modulation $\Delta_\parallel$ leading to closed quantized orbits (see Eqs. (18) and (24)). This corresponds to the situation respectively encountered in $(TMTSF)_2ClO_4$ and $(TMTSF)_2ReO_4$ under pressure on the one hand, and $(TMTSF)_2NO_3$ at ambient pressure on the other hand, as discussed in the summary section (9).

3.2. Stark–Stückelberg oscillations

Due to the modulation at wave vector $\mathbf{Q}_\perp$, one side of the FS is now made of two open sheets. In a magnetic field, the electrons travel on both sheets along the *same direction*, and possibly experience a tunnelling through magnetic breakdown from one sheet to the other. Since this tunnelling occurs in two different places (Fig. 1-b), the contributions corresponding to the two different paths may interfere. This phenomenon occurring between two LZ transitions is known as Stückelberg oscillations [30]. In the context of electronic magnetic breakdown, it has been proposed by Stark et al. to explain quantum oscillations in Mg [7], and by Uji et al. to interpret the rapid resistance oscillations in the Bechgaard salt $(TMTST)_2ClO_4$ [19,21]. We present here a quantitative picture of this effect.

Consider an electron in a magnetic field along one open sheet of the FS. During one period along the BZ, it experiences two LZ transitions to the neighbouring sheet (Fig. 1b). The tunnel probability amplitude $\sqrt{p_\perp}$ has been calculated above (12). The probability amplitude to stay on the same band is $\sqrt{1 - p_\perp}$. Therefore calling ψ_i the wave function on one sheet at one end of the BZ, the wave function ψ_f on the same sheet at the other end is:

$$\psi_f = [p_\perp e^{i\phi_B} + (1 - p_\perp)e^{i(\phi_A - 2\varphi_s)}]\psi_i \tag{13}$$

The first term corresponds to two "transmissions" from one sheet (A, see Fig. 1-b) to the neighbouring one (B), the second term corresponds to two reflections to the initial sheet (A). The phase $\phi_{A,B} = \frac{1}{\hbar}\int E_{A,B}(t)\,dt$ is the dynamical phase along the path A, B between the two MB events. The phase φ_s depends on the adiabaticity parameter δ, therefore on the amplitude of the magnetic field. It is the so-called Stokes phase accumulated at a Landau–Zener reflection: $\varphi_s = \pi/4 + \delta(\ln\delta - 1) + \arg\Gamma(1 - i\delta)$ [8]. Here, we have $2\pi\delta = B_\perp/B$. Therefore φ_s varies between 0 in the adiabatic limit ($\delta \to \infty$, absence of magnetic breakdown, $B \ll B_\perp$) to $\pi/4$ in the diabatic limit ($\delta \to 0$, strong magnetic breakdown, $B \gg B_\perp$). From (13), the probability for the electron to stay on the same sheet after one period is therefore given by:

$$|\psi_f|^2/|\psi_i|^2 = p_\perp^2 + (1 - p_\perp)^2 \tag{14}$$

$$+ 2p_\perp(1 - p_\perp)\cos(\phi + 2\varphi_s) \tag{15}$$

where $\phi = \phi_B - \phi_A$ is the magnetic-field-dependent dynamical phase accumulated between the two paths. It is given by $\phi = \frac{1}{\hbar}\int_{-t_0}^{t_0}\Delta E(t)\,dt$ with $\Delta E(t) = 2\sqrt{\Delta_\perp^2 + 4t_b^2\cos^2\frac{ev_F bBt}{\hbar}}$ and $ev_F bBt_0/\hbar = \pi/2$. In the limit, $\Delta_\perp \ll t_b$, the dynamical phase is simply given by $\phi(0) = \frac{8t_b}{ev_F bB}$. It *increases* with $\Delta_\perp$ as $\phi(\Delta_\perp) = \phi(0)F_\perp(\Delta_\perp/2t_b)$ where the function $F_\perp(x)$ is given by

$$F_\perp(x) = \int_0^{\pi/2}\sqrt{\cos^2 t + x^2}\,dt \tag{16}$$

This interference mechanism leads to oscillations of the conductivity of the form [7]:

$$\sigma_{osc} \propto 2p_\perp(1 - p_\perp)\cos(2\pi\frac{B_f}{B} + 2\varphi_s) \tag{17}$$

where the characteristic field B_f is

$$B_f(\Delta_\perp) = \frac{4t_b}{\pi ev_F b}\,F_\perp\left(\frac{\Delta_\perp}{2t_b}\right) \tag{18}$$

It *increases* with $\Delta_\perp$, since the distance between interfering orbits increases in $\mathbf{k}$ space. It is plotted in Fig. 2.

As already explained in Refs. [7,19,26], these oscillations are only visible in transport and they resemble Shubnikov–de Haas oscillations, however with a different temperature dependence. Since the dynamical phase is energy independent
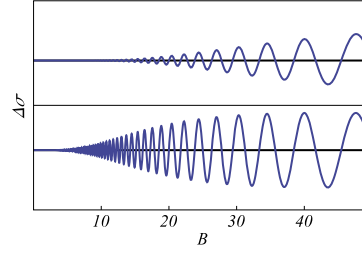
Fig. 3. Evolution of the Stark oscillations in a magnetic field (arbitrary units). Here we have taken $B_f = 250$ T, $B_\perp = 70$ T (top curve) and $B_\perp = 30$ T (bottom curve).

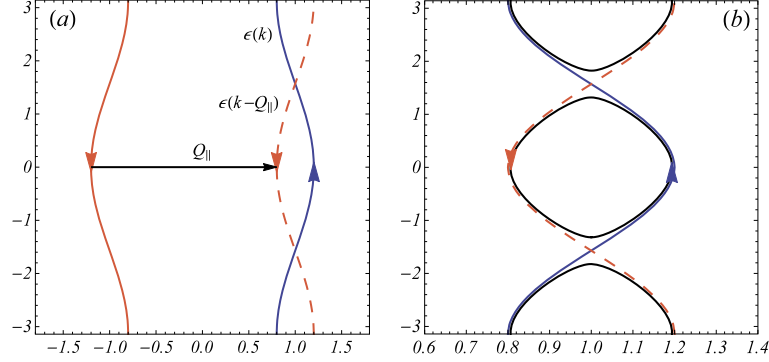**Fig. 4.** a) A modulation at a parallel wave vector $\boldsymbol{Q}_\parallel = (2k_F, 0)$ couples opposite sides of the FS. In a magnetic field, the coupled trajectories have opposite signs (blue and dashed red). b) The opening of a gap at this wavevector creates electron and hole closed pockets (black), whose motion is quantized, leading to SdH oscillations with frequency t_b. The magnetic breakdown broadens Landau levels. (For interpretation of the references to colour in this figure, the reader is referred to the web version of this article.)

(it does not depend on the position of the Fermi energy), there is no thermal damping of the oscillations. Their temperature dependence is due to that of the scattering time [19].

Since these quantum oscillations involve two LZ transitions, they vanish for a large gap $\Delta_\perp$ ($p_\perp \to 0$) and also for small gap ($p_\perp \to 1$). They vary as:

$$\sigma_{\text{osc}} \propto e^{-B_\perp/B} \left(1 - e^{-B_\perp/B}\right) \cos\left(2\pi \frac{B_f}{B} + 2\varphi_s\right) \tag{19}$$

Typical variations are shown in Fig. 3. They are maximal for $p_\perp = 1/2$, that is for a field $B_m = B_\perp / \ln 2$. This mechanism has been proposed as a possible explanation for the rapid oscillations observed in the metallic phase of (TMTSF)$_2$ClO$_4$ [19,21]. With the known physical parameters in this salt, $a = 3.65$ Å, $b = 7.7$ Å, $t_a \simeq 3000$ K, $t_b \simeq 300$ K, and a recent estimate [31] of the anion gap $\Delta_\perp \simeq 14$ meV, one finds an order of magnitude $B_\perp \simeq 40$ T that is compatible with experiments. The same mechanism should also explain the ROs in (TMTSF)$_2$ReO$_4$, which seem to be of the same nature [14]. For completion, let us mention Ref. [3], which argues that the effect is too small and proposes another mechanism related to the modulation of electron–electron scattering in the presence of a magnetic field.

4. Longitudinal ($2k_F$, 0) modulation

We now consider the existence of a longitudinal modulation with amplitude $\Delta_\parallel$ at wave vector $\boldsymbol{Q}_\parallel = (2k_F, 0)$, as it exists in (TMTSF)$_2$NO$_3$ under pressure [24,25]. This case is quite different from the previous one, since the modulation vector $\boldsymbol{Q}_\parallel = (2k_F, 0)$ couples states on *opposite* sheets of the Fermi surface (Fig. 4-a). The corresponding Hamiltonian has the form:

$$\mathcal{H}_\parallel(\boldsymbol{k}) = \begin{pmatrix} \epsilon_{\boldsymbol{k}} & \Delta_\parallel \\ \Delta_\parallel & \epsilon_{\boldsymbol{k}-\boldsymbol{Q}_\parallel} \end{pmatrix} \tag{20}$$

with

$$\epsilon_{\boldsymbol{k}-\boldsymbol{Q}_\parallel} = -\hbar v_F(k_x - k_F) - 2t_b \cos k_y b - 2t_b' \cos 2k_y b \tag{21}$$

to be compared with (3) where the modulation was at wave vector $\boldsymbol{Q}_\perp = (0, \pi/b)$. Like in the previous case, the t_b' term does not play an important role here, and we set $t_b' = 0$. The spectrum is given by

$$E_{\boldsymbol{k}} = -2t_b \cos(k_y b) \pm \sqrt{\Delta^2 + \hbar^2 v_F^2 (k_x - k_F)^2} \tag{22}$$

and the equation of the FS ($E_{\boldsymbol{k}} = 0$) is:

$$k_x = k_F \pm \frac{1}{\hbar v_F} \sqrt{4t_b^2 \cos^2 k_y b - \Delta_\parallel^2} \tag{23}$$

to be contrasted with (5) for the $\boldsymbol{Q}_\perp$ modulation. The Fermi surface is shown in Fig. 4b. It defines electron and holes pockets of equal sizes, leading to *closed* orbits in a magnetic field [32]. The area of these orbits is $\mathcal{A} = \frac{8t_b}{\hbar v_F b}$, leading to Shubnikov–de Haas oscillations with a characteristic field):

$$B_f(\Delta_\parallel) = \frac{4t_b}{\pi e v_F b} \, F_\parallel(\Delta_\parallel / 2t_b) \tag{24}$$

with

$$F_\parallel(x) = \int_0^{\arccos x} \sqrt{\cos^2 t - x^2} \, \mathrm{d}t \tag{25}$$

For a small gap, this is the same characteristic field as in the previous case. However, it *decreases* when the gap increases, since the size of the closed pockets decreases. The variation is shown in Fig. 2. It is indeed interesting to contrast the gap ($\Delta_\parallel$) dependence of the characteristic field of these SdH oscillations, with the gap ($\Delta_\perp$) dependence on the characteristic field of the Stark oscillations.

Due to magnetic breakdown, there is a finite probability of tunnelling between the closed orbits shown in Fig. 4b, leading to open orbits. To calculate this probability, we expand the Hamiltonian near a crossing point $k_y = \xi \pi / (2b) + q_y$ with $\xi = \pm 1$. It takes the form:

$$\mathcal{H}_\parallel = \begin{pmatrix} \delta + 2\xi t_b b q_y & \Delta_\parallel \\ \Delta_\parallel & -\delta + 2\xi t_b b q_y \end{pmatrix} \tag{26}$$

with the spectrum ($\delta = v_F(k_x - k_F)$)

$$E_{\boldsymbol{k}} = 2\xi t_b b q_y \pm \sqrt{\delta^2 + \Delta_\parallel^2} \tag{27}$$

In a magnetic field, there is a key difference with the previous case since the motion is *opposite* along the two sheets of the Fermi surface:

$$\hbar q_y = \pm Ft = e v_F B t \tag{28}$$

with $\hbar v_y = 2t_b b$. Therefore, the time-dependent Hamiltonian reads

$$\mathcal{H}_\parallel(t) = \begin{pmatrix} \xi v_y F t & \Delta_\parallel \\ \Delta_\parallel & -\xi v_y F t \end{pmatrix} \tag{29}$$

and the LZ probability to tunnel from one closed pocket to another is given by

$$p_\parallel = \mathrm{e}^{-\frac{B_\parallel}{B}} \quad \text{with} \quad B_\parallel = \pi \frac{\Delta_\parallel^2}{e\hbar v_y v_F} = \frac{\pi}{2} \frac{\Delta_\parallel^2}{e t_b b v_F} \tag{30}$$

This magnetic breakdown leads to a broadening of the Landau levels $E_n = (n + 1/2)e v_F b B$, which has been estimated by different methods in Refs. [33,32]. This broadening leads to a modulation of the SdH oscillations.

5. $(2k_F, \pi/b)$ nesting ordering

Like in the previous case, this modulation couples states on *opposite* sheets of the Fermi surface (Fig. 5a). The difference is that the nesting of the FS is almost perfect,[2] and the characteristic field B_f of the SdH oscillations is set by the energy scale t_b' instead of t_b. The Hamiltonian reads:

$$\mathcal{H}_N(\boldsymbol{k}) = \begin{pmatrix} \epsilon_{\boldsymbol{k}} & \Delta_N \\ \Delta_N & \epsilon_{\boldsymbol{k} - \boldsymbol{Q}_N} \end{pmatrix} \tag{31}$$
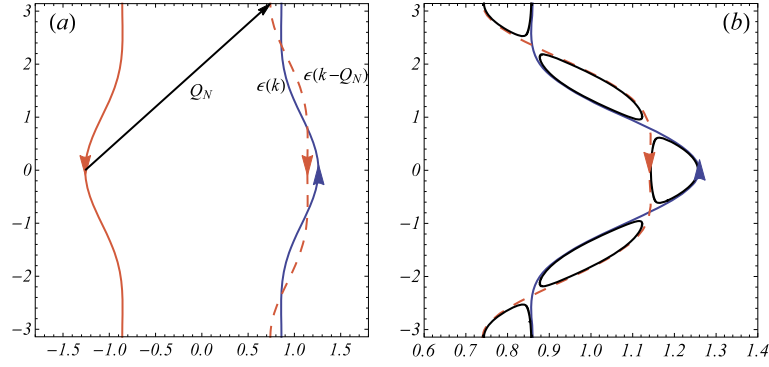
with

---

[2] See footnote 1.

Fig. 5. a) A modulation at the nesting vector $\boldsymbol{Q}_N = (2k_F, \pi/b)$ couples opposite sides of the FS. In a magnetic field, the coupled trajectories flow along opposite directions (blue and red dashed). b) The opening of a gap at this wavevector creates electronic closed pockets (black), whose motion is quantized, leading to SdH oscillations with a frequency proportional to t'_b. (For interpretation of the references to colour in this figure, the reader is referred to the web version of this article.)

$$\epsilon_{\boldsymbol{k}-\boldsymbol{Q}_N} = -\hbar v_F(k_x - k_F) + 2t_b \cos k_y b - 2t'_b \cos 2k_y b \tag{32}$$

to be compared with (3). The spectrum is given by

$$E_{\boldsymbol{k}} = -2t'_b \cos(2k_y b) \pm \sqrt{\Delta_N^2 + [\hbar v_F(k_x - k_F) - 2t_b \cos k_y b]^2} \tag{33}$$

and is shown in Fig. 5b. The equation of the FS is

$$k_x = k_F - \frac{2t_b}{v_F} \cos k_y b \pm \frac{1}{v_F} \sqrt{4t'^2_b \cos^2 2k_y b - \Delta_N^2} \tag{34}$$

The Fermi surface consists of four inequivalent small electron pockets, leading to *closed* orbits in a magnetic field. However, due to magnetic breakdown, there is a finite probability of tunnelling between these orbits, leading to larger or even open orbits. To calculate this probability, we expand the Hamiltonian near a crossing point $k_y = \xi \pi/(4b) + q_y$ with $\xi = \pm 1$. It takes the form

$$\mathcal{H}_N(\boldsymbol{k}) = \begin{pmatrix} \delta - 4\xi t'_b b q_y & \Delta_N \\ \Delta_N & \delta - 4\xi t'_b b q_y \end{pmatrix} \tag{35}$$

with the spectrum ($\delta = v_F(k_x - k_F) - t_b\sqrt{2}$)

$$E_{\boldsymbol{k}} = -4\xi t'_b b q_y \pm \sqrt{\delta^2 + \Delta_N^2} \tag{36}$$

In a magnetic field, the motion is *opposite* along the two sheets of the Fermi surface:

$$q_y = \pm Ft = e v_F B t \tag{37}$$

with $\hbar v'_y = 4t'_b b$. Therefore, the time-dependent Hamiltonian reads

$$\mathcal{H}_N(t) = \begin{pmatrix} -\xi v'_y Ft & \Delta_N \\ \Delta_N & \xi v'_y Ft \end{pmatrix} \tag{38}$$

The LZ probability to tunnel between closed orbits is therefore given by

$$p_N = e^{-\frac{B_N}{B}} \quad \text{with} \quad B_N = \pi \frac{\Delta_N^2}{\hbar v'_y F} = \frac{\pi}{4} \frac{\Delta_N^2}{e t'_b b v_F} \tag{39}$$

This tunnelling leads to a broadening of the Landau levels and to a modulation of the SdH oscillations [33]. These slow oscillations have been not observed yet in the SDW phase of Q-(TMTSF)$_2$ClO$_4$ or (TMTSF)$_2$PF$_6$.

6. Nesting ordering and transverse modulation

We consider now the case where two periodicities coexist, one at wave vector $\boldsymbol{Q}_N = (2k_F, \pi/b)$ with amplitude Δ_N, and one at wave vector $\boldsymbol{Q}_\perp = (0, \pi/b)$ with amplitude $\Delta_\perp$. This could be the case for example if a DW and a modulation due to anion ordering would coexist, as in the anion ordered phase of (TMTSF)$_2$ClO$_4$. This situation has been studied extensively in Ref. [34], and we present here a simple analytical description. It first has to be stressed that this situation *cannot* be
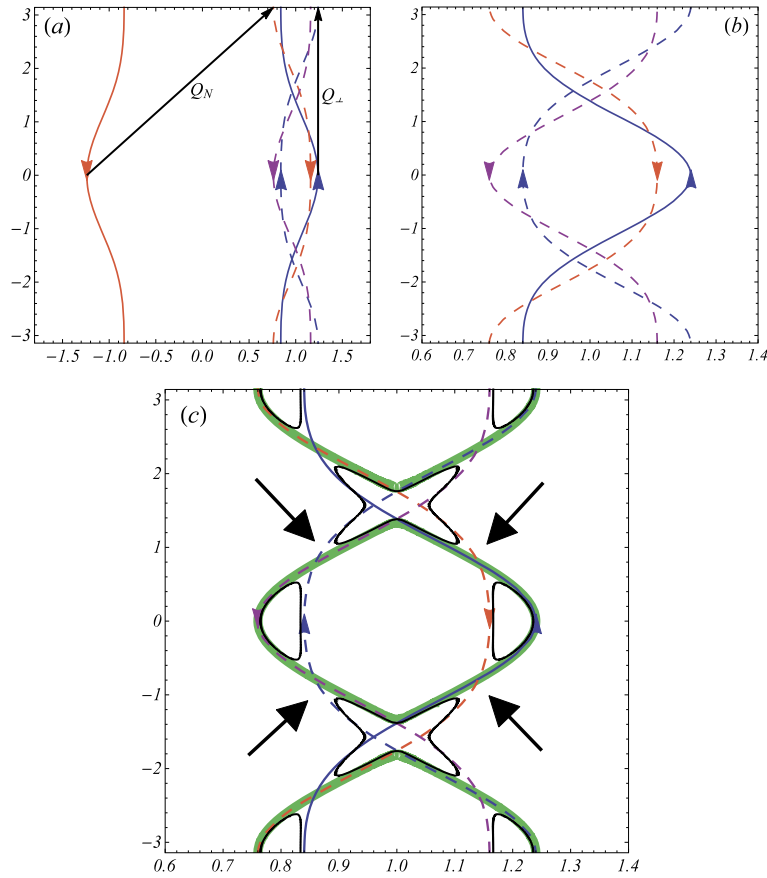
Fig. 6. a) The presence of the two modulations $\boldsymbol{Q}_N = (2k_F, \pi/b)$ and $\boldsymbol{Q}_\perp = (0, \pi/b)$ couples four states ($\boldsymbol{k}$ blue, $\boldsymbol{k} - \boldsymbol{Q}_N$ dashed red, $\boldsymbol{k} - \boldsymbol{Q}_\perp$ dashed blue and $\boldsymbol{k} - \boldsymbol{Q}_\perp + \boldsymbol{Q}_N$ dashed purple), creating six electronic closed pockets (black) (b) whose motion is quantized, leading to SdH oscillations with frequency t'_b. Notice the existence of new X-shape pockets. Magnetic breakdown through the gaps (arrows) leads to large closed orbits (shown in green in the bottom figure c) whose size is proportional to t_b. (For interpretation of the references to colour in this figure, the reader is referred to the web version of this article.)

reduced to the case of one modulation at wave vector $\boldsymbol{Q}_N - \boldsymbol{Q}_\perp$. This is a novel situation in which *four* states are coupled. Indeed these two modulations couple a state with wavevector $\boldsymbol{k}$ to an infinity of states $\boldsymbol{k} + m\boldsymbol{Q}_N + n\boldsymbol{Q}_\perp$. Considering states close to the FS, one sees that a vector $\boldsymbol{k}$ on the right side of the FS is coupled with $\boldsymbol{k} - \boldsymbol{Q}_N$, $\boldsymbol{k} - \boldsymbol{Q}_\perp$ and $\boldsymbol{k} - \boldsymbol{Q}_N + \boldsymbol{Q}_\perp$. The energy spectrum $E_{\boldsymbol{k}}$ is therefore given by the eigenvalues of the Hamiltonian:

$$
\mathcal{H}(\boldsymbol{k}) = \begin{pmatrix} \epsilon_{\boldsymbol{k}} & \Delta_{\boldsymbol{Q}_N} & \Delta_{\boldsymbol{Q}_\perp} & 0 \\ \Delta_{\boldsymbol{Q}_N^*} & \epsilon_{\boldsymbol{k}-\boldsymbol{Q}_N} & 0 & \Delta_{\boldsymbol{Q}_\perp} \\ \Delta_{\boldsymbol{Q}_\perp^*} & 0 & \epsilon_{\boldsymbol{k}-\boldsymbol{Q}_\perp} & \Delta_{\boldsymbol{Q}_N} \\ 0 & \Delta_{\boldsymbol{Q}_\perp^*} & \Delta_{\boldsymbol{Q}_N^*} & \epsilon_{\boldsymbol{k}-\boldsymbol{Q}_N+\boldsymbol{Q}_\perp} \end{pmatrix}
\tag{40}
$$

Fig. 6a shows the four states that are coupled by the modulations, with opening of a gap near $k_y = \pm\pi/(4b)$ and $k_y = \pm 3\pi/(4b)$, as seen in Fig. 6b. The new spectrum exhibits two kinds of electronic pockets: pockets with a banana shape as in the case of pure DW modulation and new pockets with a X-shape. The quantization of these orbits in a field should lead to oscillations with frequency t'_b. The important new feature here is the possibility of magnetic breakdown through four gaps, leading to closed orbits of large size, related to t_b (Fig. 6c) leading therefore to rapid quantum oscillations. The probability of having such large orbits involves four magnetic breakdowns (shown by arrows in Fig. 6c with probability p_N calculated above (Eq. (39)) and two Bragg reflections. The amplitude associated with the Bragg reflection may be more difficult to calculate, since it involves four waves instead of two. This scenario is therefore expected to lead to rapid oscillations superimposed to the slow oscillations. It naturally explains the existence of thermodynamic rapid oscillations in the FISDW of R-(TMTSF)$_2$ClO$_4$ [14,19], as well as in (TMTSF)$_2$ReO$_4$ under pressure [35,14].

7. Nesting ordering and longitudinal modulation

In this situation, two periodicities coexist, one corresponding to a DW ordering at wave vector $\boldsymbol{Q}_N = (2k_F, \pi/b)$ and a modulation at the longitudinal wave vector $\boldsymbol{Q}_\parallel = (2k_F, 0)$ as the one induced by the anion ordering in (TMTSF)$_2$NO$_3$.
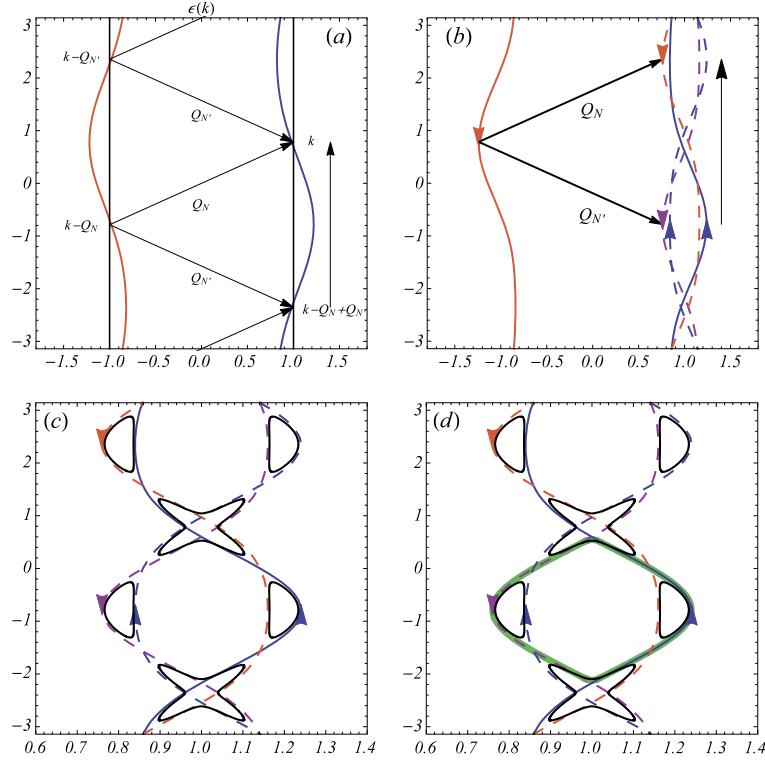
Fig. 7. Fermi surface related to the dispersion relation (42), and modulation wave vectors $\boldsymbol{Q}_N = (2k_F, \pi/2b)$ and $\boldsymbol{Q}_{N'} = (2k_F, -\pi/2b)$. a) The presence of these two modulations couples four states, couples four states ($\boldsymbol{k}$ blue, $\boldsymbol{k} - \boldsymbol{Q}_N$ dashed red, $\boldsymbol{k} - \boldsymbol{Q}_{N'}$ dashed purple and $\boldsymbol{k} - \boldsymbol{Q}_N + \boldsymbol{Q}_{N'}$ dashed blue), creating six electronic closed pockets (b) whose motion is quantized, leading to SdH oscillations with frequency t'_b. Notice the existence of new X-shape pockets. Magnetic breakdown through the gaps leads to closed orbits (green curve in d) whose size is proportional to t_b. (For interpretation of the references to colour in this figure, the reader is referred to the web version of this article.)

As in the previous case, four states are coupled close to the Fermi level, $\boldsymbol{k}$, $\boldsymbol{k} - \boldsymbol{Q}_N$, $\boldsymbol{k} - \boldsymbol{Q}_\parallel$ and $\boldsymbol{k} - \boldsymbol{Q}_N + \boldsymbol{Q}_\parallel$. This situation is therefore very similar to the previous one, since one has $\boldsymbol{Q}_\parallel = \boldsymbol{Q}_N - \boldsymbol{Q}_\perp$, and the Fermi pockets in this case resemble those presented in Fig. 6 [34]. One expects a superposition of rapid oscillations related to the large pockets due to magnetic breakdown between small pockets responsible for slow oscillations. This scenario naturally explains the two series of oscillations observed in the SDW phase of (TMTSF)$_2$NO$_3$ [22,24,25].

8. Two commensurate SDWs

The two previous sections show interesting situations when two modulations coexist. This is the case in (TMTSF)$_2$ClO$_4$ and (TMTSF)$_2$NO$_3$, where a DW modulation coexists with a modulation due to anion ordering, respectively at wave vectors $\boldsymbol{Q}_\parallel = (0, \pi/b)$ and $\boldsymbol{Q}_\perp = (2k_F, 0)$. However, rapid oscillations may also exist even in the absence of anion ordering, as it is the case in (TMTSF)$_2$PF$_6$. We now discuss another situation where two DW modulations can coexist, leading to a similar structure of the FS as in the two previous sections. Instead of the orthorhombic symmetry considered until now, we consider the triclinic symmetry pertinent to Bechgaard salts. The FS is distorted such that the two sheets are not facing each other as in the previous cases, but one is shifted with respect to the other one (Fig. 7a). Here we keep the same simple orthorhombic model where the shift is described by a phase ϕ [2]:

$$\epsilon(\boldsymbol{k}) = \hbar v_F(|k_x| - k_F) - 2t_b \cos[k_y b + \phi \, \mathrm{sgn}(k_x)] \tag{41}$$

$$- 2t'_b \cos[2k_y b + 2\phi \, \mathrm{sgn}(k_x)] \tag{42}$$

We consider the commensurate situation when the shift $\phi = \pi/4$, as shown in Fig. 7a.

Assume the existence of a modulation close to perfect nesting at wave vector $\boldsymbol{Q}_N = (2k_F, \pi/2b)$, which couples states $\boldsymbol{k}$ and $\boldsymbol{k} - \boldsymbol{Q}_N$. Consider also the modulation at wave vector $\boldsymbol{Q}_{N'} = (2k_F, -\pi/2b)$, which does not provide a so good nesting. However, the state $\boldsymbol{k} - \boldsymbol{Q}_{N'}$ is coupled with the state $\boldsymbol{k} + \boldsymbol{Q}_{N'} - \boldsymbol{Q}_N$ which is close to the FS. Therefore, we have to consider the coupling between *four* states near the Fermi level $\boldsymbol{k}$, $\boldsymbol{k} - \boldsymbol{Q}_N$, $\boldsymbol{k} - \boldsymbol{Q}_{N'}$, $\boldsymbol{k} - \boldsymbol{Q}_N + \boldsymbol{Q}_{N'}$.[3] The coupling vectors are represented in Fig. 7b.

---

[3] This is correct because $\boldsymbol{Q}_N$ and $\boldsymbol{Q}_{N'}$ obey the commensurability relation $\boldsymbol{Q}_N - \boldsymbol{Q}_{N'} = (0, \pi/b)$.

	metallic	SDW
R-ClO$_4$/ReO$_4$	$\mathbf{Q}_\perp$ (Stark, III)	$\mathbf{Q}_\perp$ and $\mathbf{Q}_N$ (VI)
NO$_3$ low pressure	$\mathbf{Q}_\parallel$ (IV)	$\mathbf{Q}_\parallel$ and $\mathbf{Q}_N$ (VII)
NO$_3$ high pressure	$\mathbf{Q}_\perp$ (III)	$\mathbf{Q}_\perp$ and $\mathbf{Q}_N$ (VI)
PF$_6$/AsF$_6$/Q-ClO$_4$		$\mathbf{Q}_N$ and $\mathbf{Q}_{N'}$ (VIII)

Fig. 8. Possible scenarios to explain the fast oscillations in the TMTSF salts. We refer to the coupling vectors associated with each scenario and the corresponding section in the paper. Here ReO$_4$ is under pressure. For NO$_3$, low and high pressure refer respectively to pressures lower and higher than 7 kbar.

Let Δ_N and $\Delta_{N'} < \Delta_N$ be the amplitude of these two modulations. The new spectrum is obtained by diagonalization of the 4×4 matrix:

$$\mathcal{H}(\mathbf{k}) = \begin{pmatrix} \epsilon_{\mathbf{k}} & \Delta_N & \Delta_{N'} & 0 \\ \Delta_N^* & \epsilon_{\mathbf{k}-\mathbf{Q}_N} & 0 & \Delta_{N'}^* \\ \Delta_{N'}^* & 0 & \epsilon_{\mathbf{k}-\mathbf{Q}_{N'}} & \Delta_N^* \\ 0 & \Delta_{N'} & \Delta_N & \epsilon_{\mathbf{k}-\mathbf{Q}_N+\mathbf{Q}_{N'}} \end{pmatrix} \qquad (43)$$

It appears clearly that this model is very similar to the one discussed in section 3, $\mathbf{Q}_N - \mathbf{Q}_{N'}$ playing the same role as $\mathbf{Q}_\perp$: four states are coupled and we have the correspondence (compare (43) with the Hamiltonian (40)):

$$\begin{aligned} \mathbf{Q}_N &= (2k_F, \pi/b) &\longleftrightarrow&& \mathbf{Q}_N &= (2k_F, \pi/2b) \\ \mathbf{Q}_\perp &= (0, \pi/b) &\longleftrightarrow&& \mathbf{Q}_N - \mathbf{Q}_{N'} &= (0, \pi/b) \\ \mathbf{Q}_N - \mathbf{Q}_\perp &= (2k_F, 0) &\longleftrightarrow&& \mathbf{Q}_{N'} &= (0, -\pi/2b) \end{aligned}$$

Like in the two previous cases, there are two kinds of closed Fermi pockets, shown on Fig. 7c, whose size is typically related to t_b' so that one should expect also slow oscillations. Magnetic breakdown through the gaps leads to large trajectories (shown in green in Fig. 7d), whose size is related to t_b and which may lead to ROs. This mechanism may actually be strengthened by Umpklapp processes due to the commensurability condition $\mathbf{Q}_N + \mathbf{Q}_{N'} = (4k_F, 0) = (2\pi/a, 0)$ as proposed by Lebed [36]. This scenario has been proposed in a qualitative form in Ref. [26]. It provides a satisfactory explanation for the ROs observed in (TMTSF)$_2$PF$_6$. In this salt, it has been found that the characteristic field B_f increases with pressure in a way that supports the proportionality between B_f and t_b [20]. The slow oscillations related to the small pockets may be difficult to observe. The ROs being due to magnetic-breakdown-induced closed orbits are also expected in magnetization experiments, but have not been observed [26].

9. Summary and discussion

Quantum oscillations in quasi-1D conductors with an open Fermi surface originate from a reconstruction of the FS due to potentials induced by periodic modulations. Their nature can be classified by their characteristic frequency – or characteristic magnetic field B_f. The frequency of the rapid oscillations is typically related to the energy t_b that describes the warping of the FS. The slow oscillations are related to the energy scale t_b' that measures the deviation from the sinusoidal warping. This paper is a review of different mechanisms that may lead to ROs. The table (Fig. 8) summarizes such mechanisms, which may explain different types of ROs in the Bechgaard salts.

- The simplest mechanisms, described in sections 3 and 4, involve only one periodic modulation.

A transverse modulation ($\Delta_\perp$) at wave vector $(2k_F, \pi/b)$ induces a pair of trajectories on the same side of the FS that may interfere via MB, and realize Stückelberg oscillations that, in the context of magnetic oscillations, have first been proposed by Stark and Friedberg [7,19,21]. This modulation is induced by anion ordering in R-ClO$_4$ at ambient pressure [37,14,19] or in ReO$_4$ under pressure [35]. The characteristic fields of the oscillations are respectively $B_f = 265$ T and $B_f = 290$ T. Due to this particular interference mechanism, these oscillations are observed solely on the conductivity, but not on thermodynamic properties.

A longitudinal modulation ($\Delta_\parallel$) at wave vector $(2k_F, 0)$ couples states on opposite sides and the reconstructed FS has closed Fermi pockets, the size of which is proportional to t_b. This is the case in NO$_3$ at ambient pressure, with the anion ordering yielding a potential at wave vector $(2k_F, 0)$ [24,25].

The evolution of the characteristic field B_f with the gap induced by the modulation may be easily calculated in these two previous scenarios (sections 3, 4). In the first case, it increases with the amplitude of the gap $\Delta_\perp$, while it decreases with the gap $\Delta_\parallel$ in the second case (Fig. 2). This is consistent with the observation of a smaller frequency in NO$_3$ at ambient pressure ($B_f = 248$ T) [24,25] compared to the cases of ClO$_4$ ($B_f = 255$–265 T) [18,37,10] or ReO$_4$ ($B_f = 320$–330 T) under pressure [35,24,25].

- More complex scenarios involve the superposition of two modulations, that is two order parameters with probably different amplitudes, a nesting modulation correlated with the apparition of a DW plus one of the two above-mentioned modulations related to an anion ordering. The reconstruction of the FS in these cases is quite rich. It exhibits closed regions with characteristic size related to size t_b' plus large trajectories induced by MB, the size of which is related to t_b. Therefore, one expects a superposition of slow and rapid oscillations. Their respective amplitude may be difficult to predict

theoretically, since it depends on the relative amplitude of the two order parameters and on the MB probability. This is the situation in R-ClO$_4$ where indeed ROs have been observed in the FISDW. It is noticeable that the ROs in the metallic phase are seen only in transport experiments, while, in the FISDW phases, they are seen both in transport and thermodynamic measurements. This proves that the mechanism for ROs is different in the presence of a single transverse modulation or in the presence of two modulations (transverse + SDW), as already noticed in Ref. [14].

• (TMTSF)$_2$NO$_3$ is a particularly rich system. Rapid and slow oscillations are observed simultaneously in the low-temperature and low-pressure SDW phase [22], compatible with the superposition of a nesting modulation plus an anion-ordering-induced modulation at wave vector $(2k_F, 0)$. The observed increase in the frequencies of both oscillation sequences is compatible with an increase in the characteristic energies t_b and t_b' under pressure [25].

However, a surprising feature is the sharp drop of the characteristic frequency of the ROs at a pressure of the order of 7 kbar from 325 T to 215 T, together with a vanishing of the slow oscillations. Such a jump is hardly understandable without an important structural change. Several arguments suggest an anion order evolving from $\mathbf{Q}_\parallel = (2k_F, 0)$ to $\mathbf{Q}_\perp = (0, \pi/b)$ around 7 kbar. Firstly, the shape of the transport anomaly passing through the anion ordering changes drastically [23,38]. Secondly, a recent investigation of the angular-dependent magnetoresistance of (TMTSF)$_2$NO$_3$ under 8.7 kbar has allowed us to conclude that a Q1D Fermi surface exists even in the presence of anion ordering [39]. Thirdly, an ab initio calculation is supporting these experimental findings [31]. These arguments suggest a pressure-induced phase transition from an anion-induced modulation at wave vector $(2k_F, 0)$ and a modulation at wave vector $(0, \pi/b)$. Therefore, the ROs reported at ≈ 8 kbar [24,25] might be actually related to Stark interferences between two sheets of folded Fermi surfaces like in R-(TMTSF)$_2$ClO$_4$. The possibility of a pressure-induced structural transition could deserve further experimental and theoretical investigations.

• The existence of ROs occurring in a SDW phase without any role played by anions, like in PF$_6$, AsF$_6$ or Q-ClO$_4$, is more problematic, since a pure SDW ordering is expected to induce only slow oscillations with frequency related to t_b'. The mechanism at the origin of such ROs may find its origin in the particular (triclinic) lattice symmetry of the Bechgaard salts. As a consequence of this triclinicity, the two sheets of the FS are actually shifted with respect to each other by a vector close to the commensurate value $(0, \pi/2b)$ so that naturally in the presence of a SDW two modulations at wave vectors $(2k_F, \pm\pi/2b)$ may coexist [26,36]. This situation is not so different from those described earlier, where a SDW and an anion-induced modulation coexist. We argue that this may explain the existence of ROs in (TMTSF)$_2$PF$_6$ or Q-(TMTSF)$_2$ClO$_4$. This scenario assumes the existence of two commensurate SDWs, at wave vectors $(2k_F, \pm\pi/2b)$, so that the coupling between relevant states at the Fermi level is described by a 4×4 matrix. One may wonder if this commensurate model is a good approximation for the actual incommensurate situation. This is probably the case and, given that the actual phase is close to commensurate, one expects that the SDW will exhibit discommensurations.

We close this conclusion by a discussion on open questions related to the commensurability of the SDW ordering in several Bechgaard salts.

Several experimental results provide hints for a commensurate SDW state in (TMTSF)$_2$PF$_6$. Strain and defect-free samples exhibit a first-order transition with a sharp increase in the resistivity at $T_{SDW} \simeq 12$ K. In addition, a non-linear conduction is the signature of a pinning mechanism due to fourfold commensurability [38]. A weakly first-order transition is also the conclusion of a study of the ^{13}C NMR linewidth through the transition [40]. Moreover signs of commensurability are also clearly provided by ^{13}C NMR spectra [41]. The examination of the ^{1}H-NMR lineshape has led to the determination of a SDW wave vector as $(\pi/a, \simeq \pi/2b)$ with a rather broad error bar for the transverse component [42,43]. This is consistent with a *triclinic* symmetry, since the best nesting vector for a simplified *orthorhombic* model would be $(\pi/a, \pi/b)$. However, the typical double horn shape of the ^{13}C-NMR spectra makes the existence of an incommensurate modulation undisputable, at least in the temperature interval between 12K and 4K [44,41].

Another puzzle concerns the anomalous behaviour in the temperature dependence of several properties in the ambient pressure SDW phases of (TMTSF)$_2$X salts. The purest samples exhibit a significant enhancement of the resistivity at 4K but, more importantly, the amplitude of ROs departs from the Lifshitz–Kosevich behaviour: it has a sudden drop at $T^\star \approx 4$ K without noticeable change in the frequency in PF$_6$, AsF$_6$ [13] and Q-ClO$_4$ [18]. Interestingly, an anomalous behaviour has also been noticed in the same temperature domain for the NMR properties, namely a sharp drop of proton [45] and ^{77}Se spin–lattice relaxation rates in (TMTSF)$_2$PF$_6$ [46] and Q-ClO$_4$ [47]. The quasi temperature-independent relaxation rate below T_{SDW} has been taken as an evidence of phason fluctuations governing the relaxation down to $T^\star$ [48,49,44]. Below that temperature, the nuclear spin relaxation slows down and exhibits an activated behaviour suggesting the opening of a gap in the SDW phason modes [45,46]. This feature is probably the signature of a fourfold commensurate SDW. An other clue in favour of commensurability is provided by microwave and radiofrequency measurements suggesting the existence below 4 K of discommensurations close to commensurability [50].

This "4 K anomaly" has not yet received any satisfactory interpretation. The exponential attenuation of the ROs below $T^\star$, without any modification of the characteristic frequency, has been interpreted as resulting from a suppression of the magnetic breakdown probability, preventing the formation of large orbits [18]. Such a hypothesis would require further ab initio band structure calculations.

However, given the remarkable sharpness of the anomaly observed by NMR [45,46,41] towards a low-temperature state characterized by an activation energy $\Delta = 10$ K [51,49], another hypothesis is that $T^\star$ marks the existence of a real phase transition between a homogeneous incommensurate SDW at high temperature and a low-temperature state comprising inclusions of commensurate SDW domains within an incommensurate background. Hence, the electronic scattering rate

might be enhanced by the existence of domain walls occurring below $T^\star$ [41]. The ROs would retain the same oscillation frequency below $T^\star$, but the scattering rate could be strongly enhanced [18].

These problems have been unsolved for about thirty years and still raise interesting open questions.

Acknowledgements

References

[1] A.G. Lebed (Ed.), The Physics of Organic Superconductors and Conductors, Springer Series in Materials Science, vol. 110, Springer, 2008.
[2] T. Ishiguro, K. Yamaji, G. Saito, Organic Superconductors, Springer, Heidelberg, 2008.
[3] A.G. Lebed, Phys. Rev. Lett. 74 (1995) 4903.
[4] L.P. Gorkov, A.G. Lebed, J. Phys. Lett. 45 (1984) L433.
[5] G. Montambaux, M. Héritier, P. Lederer, Phys. Rev. Lett. 55 (1985) 2078;
    D. Poilblanc, et al., Phys. Rev. Lett. 58 (1987) 270.
[6] V.M. Yakovenko, Phys. Rev. B 43 (1991) 11353.
[7] R.W. Stark, C.B. Friedberg, J. Low Temp. Phys. 14 (1974) 111.
[8] S.N. Shevchenko, S. Ashhab, F. Nori, Phys. Rep. 492 (2010) 1.
[9] M. Ribault, et al., J. Phys. Lett. 44 (1983) L-953.
[10] P.M. Chaikin, et al., Phys. Rev. Lett. 72 (1983) 1283.
[11] J.-P. Ulmet, et al., Solid State Commun. 58 (1986) 753.
[12] P.M. Chaikin, et al., Phys. Rev. Lett. 51 (1981) 1296.
[13] J.P. Ulmet, et al., J. Phys. Lett. 46 (1985) L-542.
[14] W. Kang, et al., Phys. Rev. B 43 (1991) 11467.
[15] T. Takahashi, D. Jerome, K. Bechgaard, J. Phys. Lett. 43 (1982) L-565.
[16] J.-P. Ulmet, P. Auban, S. Ashkenazy, Phys. Lett. A 98 (1983) 457.
[17] J.-P. Ulmet, et al., Phys. Rev. B 55 (1997) 3024.
[18] J.S. Brooks, et al., Phys. Rev. B 59 (1999) 2604.
[19] S. Uji, et al., Phys. Rev. B 53 (1996) 14339.
[20] A.V. Kornilov, et al., J. Low Temp. Phys. 142 (2006) 309;
    A.V. Kornilov, et al., Phys. Rev. B 76 (2007) 045109.
[21] S. Uji, et al., Solid State Commun. 103 (1997) 387.
[22] A. Audouard, et al., Phys. Rev. B 50 (1994) 12726.
[23] A. Mazaud, thesis, Univ. Paris-Sud, 1980.
[24] W. Kang, et al., Europhys. Lett. 29 (1995) 635.
[25] D. Vignolles, et al., Phys. Rev. B 71 (2005) 020404(R).
[26] S. Uji, et al., Phys. Rev. B 55 (1997) 12446.
[27] L.D. Landau, Phys. Z. Sowjetunion 2 (1932) 46;
    C. Zener, Proc. R. Soc. A 137 (1932) 696;
    E. Majorana, Nuovo Cimento 9 (1932) 43;
    C. Wittig, J. Phys. Chem. B 109 (2005) 8428.
[28] D. Schoenberg, Magnetic Oscillations in Metals, Cambridge Monographs in Physics, 1984.
[29] E. Blount, Phys. Rev. 126 (1962) 1636.
[30] E.C.G. Stückelberg, Helv. Phys. Acta 5 (1932) 369.
[31] P. Alemany, J.-P. Pouget, E. Canadell, Phys. Rev. B 89 (2014) 155124.
[32] J.-Y. Fortin, A. Audouard, Phys. Rev. B 80 (2009) 214407.
[33] V.M. Gvozdikov, Low Temp. Phys. 37 (2011) 964.
[34] K. Kishigi, K. Machida, J. Phys. Condens. Matter 9 (1997) 2211.
[35] H. Schwenk, et al., Phys. Rev. Lett. 56 (1986) 667.
[36] A.G. Lebed, Phys. Scr. 39 (1991) 386.
[37] X. Yan, et al., Phys. Rev. B 36 (1987) 1799.
[38] W. Kang, et al., Phys. Rev. B 41 (1990) 4862.
[39] W. Kang, O.-H. Chung, Phys. Rev. B 79 (2009) 045115.
[40] W.G. Clark, et al., private communication.
[41] S. Nagata, et al., Phys. Rev. Lett. 110 (2013) 167001.
[42] J.-M. Delrieu, et al., J. Phys. (Paris) 47 (1986) 839.
[43] T. Takahashi, Y. Maniwa, H. Kawamura, G. Saito, J. Phys. Soc. Jpn. 55 (1986) 1364.
[44] E. Barthel, et al., Europhys. Lett. 21 (1993) 87.
[45] T. Takahashi, Y. Maniwa, H. Kawamura, G. Saito, Physica B 143 (1986) 417.
[46] S. Valfells, et al., Phys. Rev. B 56 (1997) 2585.
[47] K. Nomura, et al., J. Phys. (Paris) 3 (1993) 21.
[48] W.G. Clark, et al., J. Phys. (Paris) C2 (1993) 235.
[49] W.H. Wong, et al., Phys. Rev. Lett. 70 (1993) 1882.
[50] P. Zornoza, et al., Eur. Phys. J. B 46 (2005) 223.
[51] T. Takahashi, et al., Synth. Met. 19 (1987) 225.